Advanced MRI in inflammatory arthritis

van der Leij, C.

Chapter 8

Dynamic contrast-enhanced magnetic resonance imaging using pharmacokinetic modeling. Initial experience in patients with early arthritis

Karen I. Maijer, Christiaan van der Leij, Maria J.H. de Hair, Sander W. Tas, Mario Maas, Daniëlle M. Gerlag, Paul P. Tak, Cristina Lavini

Arthritis Rheumatol. 2016;68(3):587-596.

Abstract

Objective
Analysis of dynamic contrast-enhanced magnetic resonance imaging (DCE-MRI) using pharmacokinetic modeling (PKM) provides quantitative measures that mirror microvessel integrity and can be used as an objective marker of the level of synovial inflammation. The aim of this study was to investigate the PKM parameters K^{trans}, k_{ep}, and v_e in a prospective cohort of disease-modifying antirheumatic drug (DMARD)–naive patients with early arthritis, and to validate the results by assessing their correlation with the number of synovial endothelial cells (ECs).

Methods
Forty-seven patients with early arthritis (arthritis duration <1 year, DMARD naive; comprising 14 patients with rheumatoid arthritis, 22 with unclassified arthritis, 6 with spondyloarthritis [SpA], and 5 with other arthritides) were included. At baseline, DCE-MRI was performed on an inflamed knee joint of each patient. These images were used to calculate the K^{trans} (volume transfer constant between the plasma and extracellular extravascular space [EES]), the k_{ep} (transfer constant between the EES and plasma), and the v_e (fractional volume of the EES). Second, markers of disease activity were collected. Finally, vascularity was evaluated by immunohistochemical analysis of synovial tissue samples obtained from the inflamed knee joints, using antibodies to detect von Willebrand factor (vWF), a marker of ECs.

Results
The 3 PKM parameters differed significantly between diagnostic groups at baseline, with the highest K^{trans} value being observed in patients with SpA (median 0.050/minute, interquartile range [IQR] 0.041–0.069). Furthermore, the K^{trans}, k_{ep}, and v_e values correlated significantly with markers of disease activity. Finally, the PKM parameters K^{trans} and k_{ep}, but not v_e, correlated significantly with synovial expression of vWF (r=0.647, P=0.004 for K^{trans}; r=0.614, P=0.007 for k_{ep}; r=0.398, P=0.102 for v_e).

Conclusion
These results suggest that the K^{trans}, k_{ep}, and v_e can be used to detect synovial inflammation in patients with early arthritis, and these PKM parameters may be helpful in differential diagnosis. This approach may also be useful in translational research analyzing tissue microcirculation and angiogenesis.

Introduction

Inflammatory joint diseases mainly affect the synovium and are characterized by increased tissue perfusion, capillary permeability, and angiogenesis, hypertrophy, and influx of inflammatory cells.[1-4] In the management of inflammatory joint diseases, there is a need for reliable noninvasive methods to closely monitor synovial inflammation, to predict the diagnosis, and, finally, to predict a patient's prognosis with respect to the future development of bone destruction.[5] However, conventional methods, such as clinical examination and radiography, do not allow detailed evaluation of synovial inflammation.[6,7]

Dynamic contrast-enhanced magnetic resonance imaging (DCE-MRI) is an MRI technique consisting of the time-dependent registration of changes in the MR signal intensity during and after an intravenous bolus injection of a gadolinium (Gd)–based contrast agent. The resulting time–intensity curve can be post-processed to produce descriptive parameters such as the rate of (early) enhancement and the maximum enhancement, or to produce heuristic parameters such as the shape of the time–intensity curve.[8] With a quantitative approach, it is also possible to obtain physiology-related parameters by converting the time–intensity curves to concentration–time curves, and subsequently fitting these data with pharmacokinetic models (PKMs) such as the Tofts model.[9] In patients with rheumatoid arthritis (RA), descriptive DCE-MRI parameters are correlated with clinical disease activity parameters such as the erythrocyte sedimentation rate (ESR) and C-reactive protein (CRP) level,[10-12] as well as with histologic measures of inflammation such as vascularity and perivascular edema.[11,13-16] Furthermore, these descriptive parameters have been shown to be predictive of the progression of erosive disease,[17] and have been found to decrease after successful treatment.[18-22] Therefore, DCE-MRI parameters have been suggested to represent potential objective markers of synovial inflammation.

Analysis of DCE-MR images using descriptive parameters has, however, some significant disadvantages. Parameters such as the maximum enhancement or slope reflect signal changes that occur when monitoring contrast uptake, but these are dependent on the scanner parameters and field strength. These parameters are therefore unsuitable to compare studies that are based on data acquired with different scanners or with different MRI settings. For this reason, the use of physiology-related parameters that are obtained by means of PKM is preferred. These models should provide absolute measures of the microvessel integrity, such as the K^{trans} (the volume transfer constant between the plasma and extracellular extravascular space [EES]), the v_e (the fractional volume of the EES), the k_{ep} (the transfer constant between the EES and plasma), and the v_p (the plasma volume).[9] Besides being used as objective markers of synovial inflammation, pharmacokinetic DCE-MRI parameters can also be used for research into certain aspects of tissue microcirculation[23,24] and for assessment of treatment by monitoring microvascular changes.[25,26]

In this study, we investigated the PKM parameters K^{trans}, k_{ep}, and v_e in a prospective cohort of disease-modifying antirheumatic drug (DMARD)–naive patients with early arthritis. Since the K^{trans} and v_e provide absolute measures of the microvessel integrity, we validated our results by assessing their correlation with synovial expression of the endothelial cell (EC) marker von Willebrand factor (vWF).

Patients and methods

Study subjects

The study included patients enrolled between March 2004 and April 2009 in a prospective early arthritis cohort, the Synoviomics cohort of the Academic Medical Center (AMC) at the University of Amsterdam (Amsterdam, The Netherlands), for whom DCE-MRI data from an inflamed knee joint were available (n = 54).[27] All patients had the disease for under 1 year, as measured from the first clinical evidence of joint swelling. At the time of inclusion, all patients had active arthritis in at least 1 knee joint, and all patients were DMARD naive. The study was approved by the Medical Ethics Committee of the AMC and was performed in accordance with the Declaration of Helsinki. All patients gave written informed consent.

Study design

At baseline, demographic information as well as the following clinical and laboratory parameters were collected. The tender joint count (of 68 joints assessed), swollen joint count (of 66 joints assessed), and Disease Activity Score in 28 joints (DAS28)[28] were obtained. In addition, the amount of swelling of the knee joint was assessed by the operating physician in synovial tissue from the biopsied joint (score range 0–3, where 0 indicates no swelling and 3 indicates severe swelling). IgM rheumatoid factor (IgM-RF) levels were determined using a Sanquin IgM-RF enzyme-linked immunosorbent assay (ELISA) kit (with the upper limit of normal [ULN] defined as 12.5 IU/ml) until December 2009, and thereafter using a Hycor Biomedical IgM-RF ELISA kit (with the ULN defined as 49 IU/ml). Anti–citrullinated protein antibodies were measured using an anti–cyclic citrullinated peptide 2 ELISA (with the ULN defined as 25 kAU/liter) (CCPlus; Eurodiagnostica). Finally, the ESR (in mm/hour), CRP level (in mg/liter), and radiographs of the hands and feet were obtained.

A diagnosis was made at baseline in each patient. After follow-up, patients were reclassified on the basis of the 2-year clinical diagnosis, determined according to the cumulative fulfilment of standard classification criteria for established rheumatic diseases, and patients who did not fulfil these criteria were designated as having unclassified arthritis (UA) (phase e, according to the European League Against Rheumatism [EULAR] Study Group for Risk Factors for Rheumatoid Arthritis).[29-35]

Furthermore, after 2 years of follow-up, patients with early arthritis fulfilling the American College of Rheumatology (ACR)/EULAR 2010 criteria for RA[29] were classified according to arthritis outcome, as follows: 1) self-limiting disease, defined as no arthritis on examination and no treatment with DMARDs or steroids in the preceding 3 months; 2) persistent nonerosive disease, defined as the presence of arthritis in at least 1 joint and/or treatment with DMARDs or steroids in the preceding 3 months and no signs of erosions on conventional radiographs; or 3) erosive disease, defined as the presence of joint erosions on radiographs of the hands and/or feet.[36]

MRI

At baseline, DCE-MRI of an inflamed knee of each patient was performed. Images were acquired on a 1.5T MRI scanner (Signa Horizon Echospeed, LX9.0; General Electric Medical Systems). Patients were placed in a supine position with the knee joint centered in the magnetic field in a dedicated extremity coil (quadrature detection). The DCE-MRI data were acquired using an axial T1-weighted 3-dimensional fast spoiled gradient-echo (FSPGR) sequence (echo time 4.6 msec, repetition time 8.1 msec, flip angle 30°, field of view 180 × 180 × 80 mm, voxel size 1.4 × 1.4 × 4 mm, acquisition time per volume 21 seconds, 20 dynamic scans). Before the DCE-MRI protocol, a series of FSPGR sequences (same parameters as described above, but using only 1 dynamic scan) were run with variable flip angles (theta values of 5°, 10°, 20°, or 30°) in order to provide data to determine absolute precontrast T1 maps.
During the DCE-MRI examination, patients were given a gadopentetate dimeglumine contrast agent (Magnevist; Bayer) at a dose of 0.1 mM/kg body weight, delivered by means of a pump at a speed of 3–5 mM/second. Delivery of the contrast agent was followed by a chase bolus of 12–20 ml of 0.9% NaCl. Because the knee joint was carefully fixed and padded within the coil, movement during the scan was minimal. Therefore, no image registration was performed on the dynamic scan.

Pharmacokinetic modeling

Data were analyzed off-line using in-house software (Dynamo).[8] First, the absolute precontrast T1 maps were calculated by fitting the data obtained with the variable flip angle FSPGR sequences. The signal intensities were transformed into signal concentrations (in each voxel) using the precontrast T1 maps. The Gd concentration–time relationship, or $C_{Gd}(t)$, was then calculated according to the following equation (Equation 1)

$$C_{Gd}(t) = -\frac{1}{TR \cdot \Re_1}\left\{\ln\left(\frac{SE(t)\cdot\left(e^{-\frac{TR}{T_{10}}}-1\right)+e^{-\frac{TR}{T_{10}}}\left(1-\cos\vartheta\right)}{1+\cos\vartheta\left(SE(t)\left(e^{-\frac{TR}{T_{10}}}-1\right)-1\right)}\right)-\frac{TR}{T_{10}}\right\} \quad \text{Eq. (1)}$$

where r1 represents the tissue relaxivity constant of proportionality between the Gd concentration and increase in relaxation rate (we used an r_1 value of 4.52 lt/second/m*M*), *SE*(*t*) represents the signal enhancement at time *t*, calculated as *(SE(t)=(S(t)-S(0))/S(0))* with t_0 being the time before contrast enhancement, and T10 represents the native T1 (the value before contrast enhancement).[37]

Thereafter, we applied the Tofts model in its extended form, calculated with the following equation (Equation 2)

$$C_t(t) = v_p C_p(t) + K_{trans} \cdot C_p(t) \otimes e^{-\frac{K^{trans}}{v_e}t} \quad \text{Eq. (2)}$$

where $C_t(t)$ is the tissue signal concentration at time *t* (as calculated with Equation 1), v_p is the fractional volume of the plasma, v_e is the fractional volume of the EES, and $C_p(t)$ is the arterial input function (AIF), i.e., the estimated plasma concentration of contrast agent in the capillaries feeding the tissue.[9]

In order to measure the AIF, we manually selected a region of interest (ROI) in the popliteal artery in multiple sections of the scan. An arterial concentration–time curve, the $C_{blood}(t)$, was obtained using Equation 1, and using a T_{10}*Blood* value of 1,540 msec.[38] Plasma concentrations in the capillary (C_p) were estimated using the equation $C_p = C_{blood}/(1-Hct)$, where *Hct* represents the hematocrit constant (assigned a value of 0.45).[38]

To avoid partial volume effects, only the pixels with the highest enhancement were used to generate the arterial signal. Because of the low time resolution of the dynamic scan, the AIF needed adjustment before being used for the PKM analysis. The AIF was shifted and its peak amplitude corrected according to a previously published method.[39] The resulting plasma concentration–time curve, the $C_p(t)$, was fitted to the following formula (Equation 3)

$$C_p(t) = \beta\left(\chi \cdot t \cdot e^{-mb\cdot t} - e^{-mb\cdot t} + e^{-ma\cdot t}\right) \quad \text{Eq. (3)}$$

which provided the $C_p(t)$ curve a functional form that would allow Equation 2 to be solved in closed form.[40] The concentration in the tissue (C_{tiss}) then could be calculated with the following equation (Equation 4)

$$C_{tiss}(t)=\beta\left\{v_i\left(\chi\cdot t\cdot e^{-mbt}-e^{-mbt}+e^{-mat}\right)+\right. \quad \text{Eq. (4)}$$
$$\left.+v_e k_{ep}\left[\frac{\chi}{k_{ep}-mb}\left(t\cdot e^{-mbt}-\frac{\left(e^{-mbt}-e^{-k_{ep}\cdot t}\right)}{k_{ep}-mb}\right)+\frac{(e^{-mat}-e^{-k_{ep}\cdot t})}{k_{ep}-ma}-\frac{\left(e^{-mbt}-e^{-k_{ep}\cdot t}\right)}{k_{ep}-mb}\right]\right\}$$

The descriptors have been described previously in reference 40 (in which Equation 3 and Equation 7 are identical in form to Equation 3 and Equation 4 in the present study). The PKM parameters K^{trans}, v_e, and k_{ep} (K^{tran}/v_e) were determined by fitting Equation 4 to the calculated concentration–time curves in the tissue and using the patient-specific AIF, as described above. Nonlinear fitting was done on a voxel-by-voxel basis, using the Levenberg-Marquardt fitting algorithm in the Matlab platform (Mathworks).

Selection of the ROIs and the ROI-specific PKM parameters

An ROI excluding enhancing (muscle) tissue was manually drawn by a trained investigator (CvdL) on maps showing the maximum enhancement. This was done in 12 adjacent levels, using the tibial plateau as the distal landmark.
Bones were automatically segmented and excluded from the ROIs using the precontrast T1 signal intensity, leaving the synovium within the ROI (Figure 8.1). Within these 3-dimensional ROIs, the median values for the distribution of the PKM parameters (K^{trans}, k_{ep}, and v_e) were calculated.

PKM exclusion criteria

The quality of the K^{trans} maps was not always consistent. As the analysis was done on a pixel-by-pixel basis, and because of the sensitivity of the fitting procedure to noise, the PKM parameters were not calculated on pixels that had a noise in the time–intensity curve that exceeded 30% of the average baseline (precontrast) values. If the amount of pixels excluded was >30%, the patient was not included in the study. Furthermore, patients were excluded if the T1 map calculated from the variable flip angle method was unreliable, or if it was not possible to extract a good AIF in the field of view.

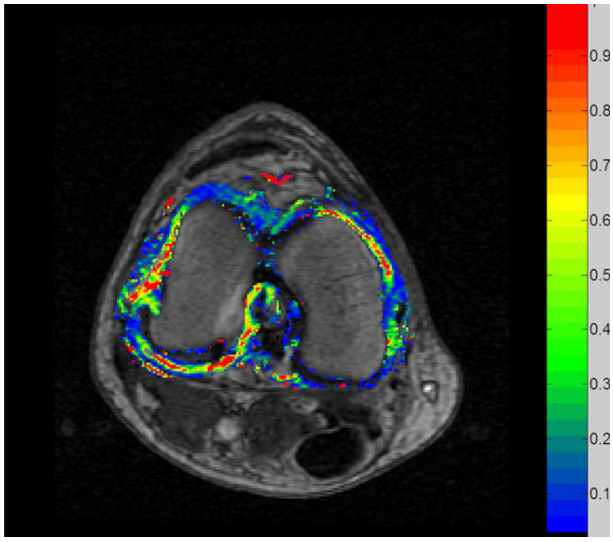

Figure 8.1 A representative image of the knee joint of a patient with early arthritis, as assessed by dynamic contrast-enhanced magnetic resonance imaging (DCE-MRI). The map shows the K^{trans} values (the volume transfer constant between the plasma and extracellular extravascular space) in the segmented region of interest (the synovium), superimposed on a T1-weighted image of the DCE-MRI scan. The concentration–time curves as well as the fitted model are shown for 2 pixels with low and high K^{trans} values.

Collection of synovial biopsy tissue, immunohistochemical staining, and quantification of ECs

At baseline, all study subjects underwent arthroscopic synovial biopsy sampling, as previously described.[41,42] The synovial tissue was harvested from the same inflamed knee joint on which the DCE-MRI had been performed at a maximum of 1 week before the biopsy.[43] To correct for sampling error, at least 6 biopsy specimens were collected for immunohistochemical analysis, as has been described previously.[44] The synovial tissue was snap-frozen en bloc in Tissue-Tek OCT medium (Sakura Finetek Europe) immediately after collection. Cryostat sections (5 µm each) were cut and mounted on Star Frost adhesive glass slides (Knittelglass). Sealed slides were stored at −80°C until further used. For detection of ECs, synovial tissue sections were stained using monoclonal antibodies to vWF (F8/86; Dako).[45]

Statistical analysis

Categorical data were depicted as the number (%), while non–normally distributed variables were depicted as the median (interquartile range [IQR]) or as the median (range) when ≤3 patients were analyzed. In comparing the PKM parameters between

the different diagnostic groups at baseline or between the different arthritis outcome groups (self-limiting disease, persistent nonerosive disease, or erosive disease), the Kruskal-Wallis test was used when >2 groups were compared. Bivariate correlations of non–normally distributed variables were analyzed using Spearman's rank correlation test. All statistical analyses were performed using SPSS software (version 20.0; IBM). P values less than or equal to 0.05 were considered statistically significant.

Results

Characteristics of the patients

Baseline characteristics of the patients with early arthritis are shown in Table8. 1. Of the 54 patients, 1 was excluded because the data could not be fitted to the PKM models (met the PKM exclusion criterion), 2 were excluded based on the AIF, and 4 were excluded based on the T1 map. At baseline, of the remaining 47 patients with early arthritis, 14 were classified as having RA, 22 as having UA, 6 as having spondyloarthritis (SpA), and 5 as having other arthritides. The other arthritides group consisted of 2 patients with gout, 2 patients with inflammatory osteoarthritis, and 1 patient with systemic lupus erythematosus. The overall disease duration at baseline was a median of 2 months (IQR 1–6 months). Of the 22 patients who were initially classified as having UA, 4 fulfilled the ACR/EULAR 2010 criteria for RA after 2 years of follow-up, 16 remained unclassified, and 2 were classified as having SpA after 2 years of follow-up.

Of the total of 18 patients who fulfilled the ACR/EULAR 2010 criteria for RA after 2 years of follow-up, 3 patients had self-limiting disease, 5 patients had persistent nonerosive disease, and 3 patients had erosive disease, while for 7 patients, the arthritis outcome data were not available, and these patients were therefore excluded from the arthritis outcome analysis.

Table 8.1 Baseline demographic and clinical characteristics of the study patients with early arthritis (n=47).

Sex, no. (%) female	23 (49)
Age, median (IQR) years	47 (36–56)
IgM-RF positive, no. (%)	11 (23)
ACPA positive, no. (%)	9 (19)
IgM-RF and ACPA positive, no. (%)	6 (13)
ESR, median (IQR) mm/hour	17 (7–36)
CRP, median (IQR) mg/liter	5.6 (1.7–21.3)
Swelling of biopsied joint, median (IQR) score (scale 0–3)	1 (1–2)
DAS28, median (IQR)	3.91 (2.80–5.18)
68-joint TJC, median (IQR)	3 (1–14)
66-joint SJC, median (IQR)	2 (1–5)

IQR = interquartile range; IgM-RF = IgM rheumatoid factor; ACPA = anti–citrullinated protein antibody; ESR = erythrocyte sedimentation rate; CRP = C-reactive protein; DAS28 = Disease Activity Score in 28 joints; TJC = tender joint count; SJC = swollen joint count.

DCE-MRI PKM parameters in different diagnostic and arthritis outcome groups

To evaluate potential differences in microvessel integrity between the different baseline diagnoses and between the different arthritis outcome groups (self-limiting disease, persistent nonerosive disease, or erosive disease), we compared the PKM parameters in those groups. We observed a significant difference in the PKM parameters K^{trans} and k_{ep} between the different groups classified according to diagnosis at baseline (P=0.026 for K^{trans}, P=0.024 for k_{ep}, and P=0.094 for v_e) (Figures 8.2A–C). The K^{trans} value was highest in patients with SpA (median 0.050/minute, IQR 0.041–0.069) and lowest in those with other arthritides (median 0.003/minute, IQR 0.000–0.036). Intermediate K^{trans} values were obtained in the DCE-MR images from patients with UA (median 0.028/minute, IQR 0.015–0.042) and from those with RA (median 0.026/minute, IQR 0.008–0.044) (see Supplementary Table S8.1, available on the Arthritis & Rheumatology web site at http://onlinelibrary.wiley.com.ezproxy.ub.unimaas.nl/doi/10.1002/art.39469/abstract).
This analysis was followed by the investigation of PKM parameters in relation to arthritis outcome (self-limiting, persistent nonerosive, or erosive disease) in patients fulfilling the ACR/EULAR 2010 criteria for RA after 2 years of followup. The K^{trans} value was highest in the persistent nonerosive disease group (median 0.041/minute, IQR 0.024–0.045) and lowest in the self-limiting disease group (median 0.006/minute, range 0.005–0.022). Intermediate K^{trans} values were obtained in images from patients with erosive disease (median 0.027/minute, range 0.000–0.083) (see Supplementary Table S8.1, available on the Arthritis & Rheumatology web site at http://onlinelibrary.wiley.com.ezproxy.ub.unimaas.nl/doi/10.1002/art.39469/abstract). However, none of the PKM parameters showed a statistically significant difference between the different arthritis outcome groups (P=0.212 for K^{trans}, P=0.262 for k_{ep}, and P=0.357 for v_e). Taken together, these data indicate that the PKM parameters K^{trans}, k_{ep}, and v_e may be useful in classifying patients according to diagnosis in the early phase of inflammatory joint diseases.

Correlations of DCE-MRI PKM parameters with local and systemic disease activity markers in patients with early arthritis

To evaluate the PKM parameters as markers of disease activity in inflammatory joint diseases, we correlated them with local and systemic markers of disease activity. We found a statistically significant correlation between the PKM parameters and the severity of swelling of the biopsied joint as assessed by the operating physician (r=0.505, P<0.001 for K^{trans}; r=0.456, P=0.001 for k_{ep}; and r=0.500, P<0.001 for v_e).

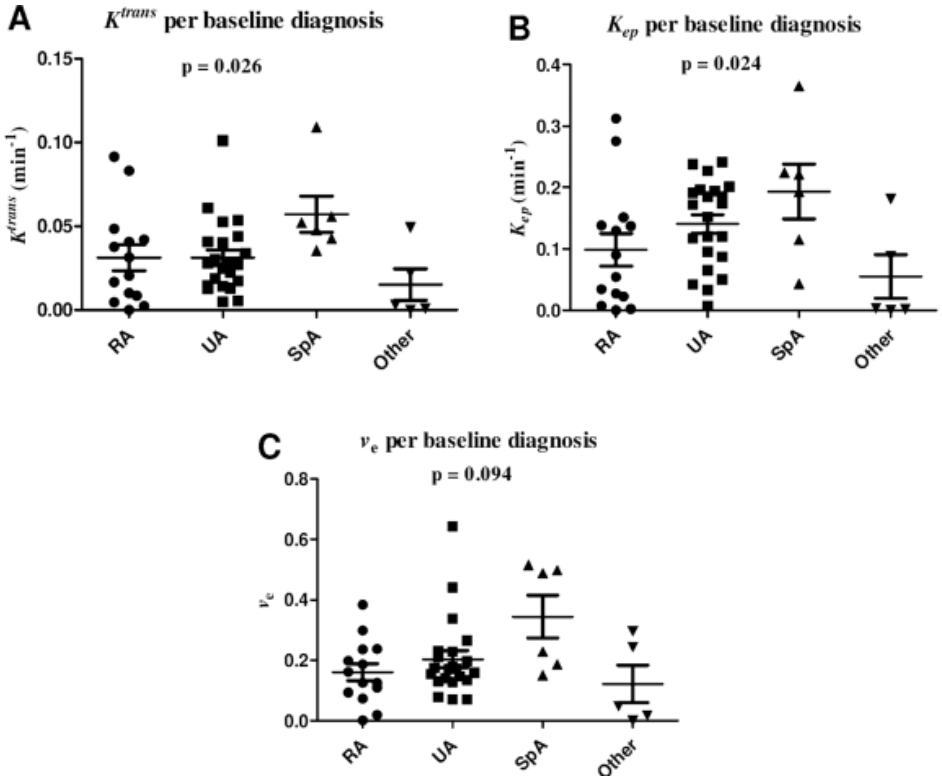

Figure 8.2 Baseline pharmacokinetic modeling (PKM) parameters from dynamic contrast-enhanced magnetic resonance imaging in relation to different diagnoses in patients with early arthritis. The PKM parameters K^{trans} (volume transfer constant between the plasma and extracellular extravascular space [EES]) (A), k_{ep} (transfer constant between the EES and plasma) (B), and v_e (fractional volume of the EES) (C) were assessed in patients who were classified as having rheumatoid arthritis (RA), unclassified arthritis (UA), spondyloarthritis (SpA), or other arthritides at baseline. The Kruskal-Wallis test was used for group comparisons. Symbols represent individual patients; bars show the median and interquartile range.

Furthermore, all PKM parameters correlated significantly with the CRP levels as a systemic marker of disease activity (r=0.412, *P*=0.004 for K^{trans}; r=0.295, *P*=0.046 for k_{ep}; and r=0.316, *P*=0.032 for v_e). There was no significant correlation of any of the PKM parameters with the DAS28 (r=0.375, *P*=0.126 for K^{trans}; r=0.377, *P*=0.123 for k_{ep}; and r=0.318, *P*=0.198 for v_e), and only the v_e was significantly correlated with the ESR (r=0.286, *P*=0.054 for K^{trans}; r=0.417, *P*=0.085 for k_{ep}; and r=0.525, *P*=0.025 for v_e) (Figures 8.3A–C).

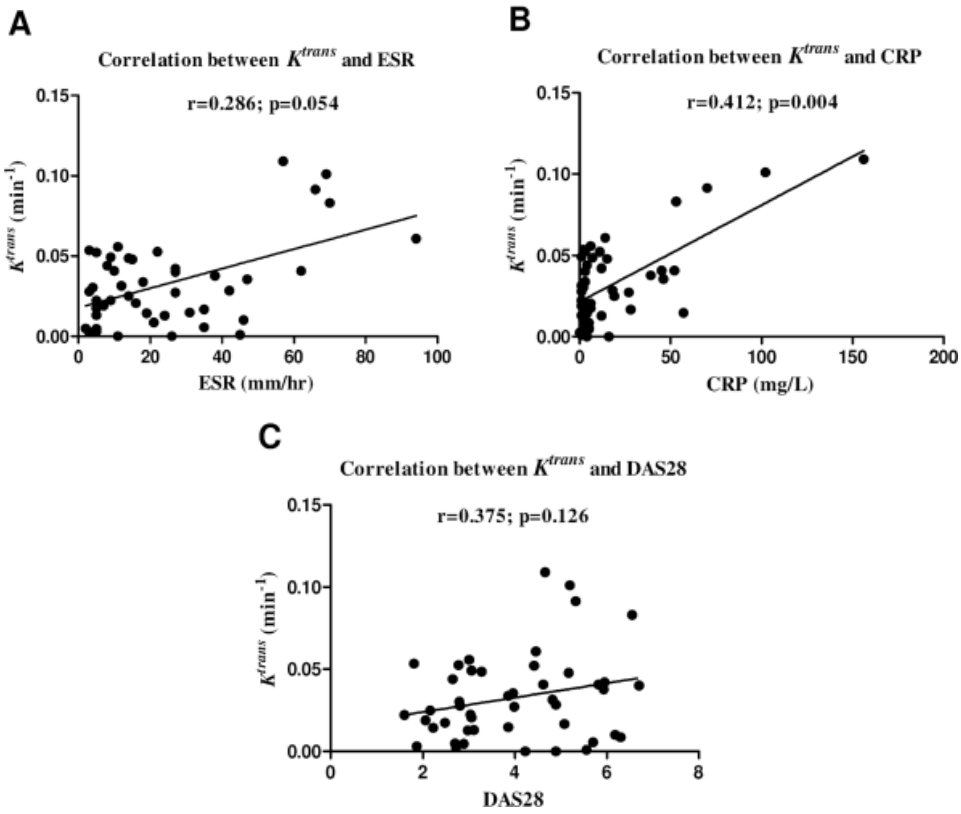

Figure 8.3 Correlations of the dynamic contrast-enhanced magnetic resonance imaging pharmacokinetic parameter K^{trans} and systemic markers of disease activity at baseline in patients with early arthritis. Correlations between the K^{trans} and erythrocyte sedimentation rate (ESR) (A), K^{trans} and C-reactive protein (CRP) level (B), and K^{trans} and Disease Activity Score in 28 joints (DAS28) (C) were analyzed using Spearman's rank correlation test.

Correlation of the K^{trans} with synovial tissue expression of vWF

In order to validate the use of PKM parameters reflecting the microvessel integrity as objective markers of synovial inflammation, we studied the correlation of these parameters with the number of synovial blood vessels. Based on the availability of synovial tissue of good quality, 18 individuals could be included in this analysis. The PKM parameters K^{trans} and k_{ep} each correlated significantly with synovial expression of vWF (r=0.647, P=0.004 for K^{trans} and r=0.614, P=0.007 for K_{ep}) (Figure 8.4), whereas the parameter v_e was not significantly correlated with the expression of vWF (r=0.398, P=0.102). These data demonstrate that the PKM parameters mirror the number of synovial ECs.

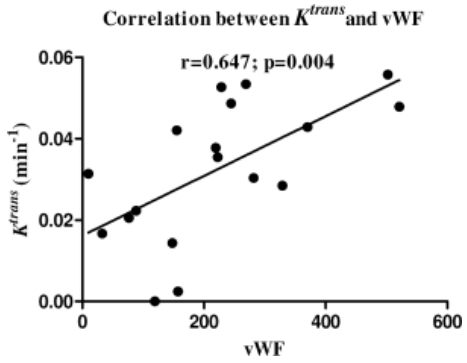

Figure 8.4 Correlations of the dynamic contrast-enhanced magnetic resonance imaging pharmacokinetic parameter K^{trans} and the expression of the endothelial cell marker von Willebrand factor (vWF) in the synovial tissue of patients with early arthritis. Correlations were analyzed using Spearman's rank correlation test.

Discussion

This is the first study investigating the value of DCE-MRI PKM parameters (K^{trans}, k_{ep}, and v_e) in the Tofts model, each of which represents an absolute measure of microvessel integrity, in a prospective cohort of DMARD-naive patients with early arthritis. Our results show that K^{trans}, k_{ep}, and v_e differ between diagnostic groups and correlate with local and systemic markers of disease activity. Importantly, we validated our results by demonstrating that these parameters are correlated with the expression of the EC marker vWF in synovial biopsy tissue from the same joint. Taken together, these data suggest that PKM parameters have value in differentiating patients with a different inflammatory joint disease diagnosis. In addition, this approach can be used to detect synovial inflammation, and may be helpful in investigating certain aspects of tissue microcirculation and angiogenesis.

Research on the relationship between DCE-MRI PKM parameters and aspects of the disease is relatively new in the arthritis field. Qualitative DCE-MRI analysis has been applied in early arthritis,[46] while its value has been proven in distinguishing between malignant and benign musculoskeletal lesions and other tumors.[47-52] Extensive evidence has been presented to support the value of PKM analysis in patients with cancer.[53] Since the inflamed synovium exhibits the same features as those found in malignant tumors, such as increased tissue perfusion, increased capillary permeability, and invasive growth of the synovial tissue into bone and cartilage, we hypothesized that PKM parameters may also be of use in the diagnostic and/or prognostic classification of arthritis patients. Indeed, we found that the K^{trans}, k_{ep}, and v_e were significantly different between diagnostic groups, with the highest values in patients with SpA. This is

consistent with the findings in earlier studies showing a significantly higher microvessel density in the synovial tissue from SpA patients with active inflammation compared to controls or patients with other forms of arthritis, such as RA.[54,55] The data presented herein support the rationale for future studies to confirm the value of PKM parameters for differential diagnosis.

Since the K^{trans}, k_{ep}, and v_e correlated significantly with the severity of swelling of the joint, with the highest values for the severity of swelling observed in patients with SpA (see Supplementary Table S8.2, available on the Arthritis & Rheumatology web site at http://onlinelibrary.wiley.com.ezproxy.ub.unimaas.nl/doi/10.1002/art.39469/abstract), the K^{trans}, k_{ep}, and v_e may be more representative of local inflammation than of a specific diagnosis. Another potential caveat is the fact that the K^{trans}, k_{ep}, and v_e were analyzed using the whole 3-dimensional image of the synovium (and not only in regions of high K^{trans}), resulting in the median values being shifted toward lower values. It is possible that a better depiction of the diagnosis could be represented by averaged values in the most affected area of the synovium. This hypothesis needs further testing.

The K^{trans}, k_{ep}, and v_e significantly correlated with local markers of disease activity and with CRP levels. However, these PKM parameters did not correlate with other systemic markers of inflammation, such as the DAS28 and ESR. Perhaps this is not surprising, as we only examined a single knee joint of patients with mostly systemic polyarticular diseases.

Earlier studies showed that the synovial vasculature is related to disease progression.[48,50] In our study, we did not find a correlation between PKM parameters and arthritis outcome (self-limiting, persistent nonerosive, or erosive disease) in patients fulfilling the ACR/EULAR 2010 criteria for RA after 2 years of followup. These results need to be interpreted with caution, as we could only evaluate the outcome in a small number of patients (3 with self-limiting disease, 5 with persistent nonerosive disease, and 3 with erosive disease).

The PKM parameter K^{trans} represents the transfer constant of the contrast agent between the plasma space and the extracellular space, and the value increases in an environment of high capillary permeability (although the K^{trans} is not a direct measure of permeability). The results of our study show a clear correlation with the expression of vWF in the synovial tissue from the same joint, which is consistent with findings of increased permeability in newly formed vessels due to neoangiogenesis in tumor tissue.[56] It has been suggested that the number of blood vessels is significantly increased in RA patients whose disease is longstanding, and this is correlated not only with higher disease activity and severity, but also with increased inflammatory cell infiltration.[1] Taken together, the findings indicate that increased angiogenesis is considered an important factor in the pathogenesis of RA[57] and also in other inflammatory joint diseases such as SpA. Based on our results, the K^{trans} is a noninvasive marker of synovial angiogenesis in patients with early arthritis.

Despite the advantages of PKM compared to descriptive parameters in DCE-MRI, one significant limitation is that its implementation is far from straightforward. The absolute contrast agent concentrations must be calculated from the MR signal, a process that requires additional scans, and the AIF needs to be either measured or approximated. In both cases, potential errors are introduced. In our study, a low temporal resolution (21 seconds) was used to favor spatial resolution and coverage of the whole knee, and a correction method was therefore needed to estimate the AIF. The calculation of the contrast agent concentration is hampered by the fact that some constants, such as the hematocrit, relaxivity, and blood T1 constants, have not been measured, and therefore values from the literature have been used. All this contributes to the inaccuracy of the PKM parameters.[58]

Moreover, noise and inadequate temporal resolution severely limit the robustness of the (nonlinear) fitting procedure: it is thus important to exclude pixels that are not suitable for fitting. A thorough optimization of the protocol is essential to ensure sufficient signal-to-noise ratio. The standardization of the infusion technique is also important. To control for variability as much as possible, we standardized several parameters in our study, such as the diameter of the needle and duration of the infusion. Although routine use of this model in clinical practice may be challenging due to these limitations, we think it is feasible to implement DCE-MRI PKM in clinical practice in specific cases.

Taken together, our results indicate that the DCE-MRI PKM parameters K^{trans}, k_{ep}, and v_e are thought to provide absolute measures of microvessel integrity, allowing comparison between patients and between studies, and therefore offering a great advantage over the use of DCE-MRI descriptive parameters. We demonstrated that these PKM parameters correlated with the expression of the EC marker vWF in synovial tissue from patients with early arthritis, which can be of use in the context of translational research bridging aspects of tissue microcirculation and angiogenesis with advanced imaging techniques. Our results also suggest that the K^{trans}, k_{ep}, and v_e can be used as diagnostic biomarkers in early inflammatory joint disease. Finally, these PKM parameters may be used to detect synovial inflammation in patients with early arthritis, which could facilitate the evaluation of joints inaccessible to proper clinical examination or joints with suspected, but not definite, synovitis or the detection of subclinical synovitis in patients at risk of developing RA.

References

1. Izquierdo E, Canete JD, Celis R, Santiago B, Usategui A, Sanmarti R, et al. Immature blood vessels in rheumatoid synovium are selectively depleted in response to anti-TNF therapy. PLoS One 2009;4:e8131.
2. Szekanecz Z, Besenyei T, Szentpetery A, Koch AE. Angiogenesis and vasculogenesis in rheumatoid arthritis. Curr Opin Rheumatol 2010;22:299–306.
3. Tak PP, Thurkow EW, Daha MR, Kluin PM, Smeets TJ, Meinders AE, et al. Expression of adhesion molecules in early rheumatoid synovial tissue. Clin Immunol Immunopathol 1995;77:236–42.
4. Tak PP, Smeets TJ, Daha MR, Kluin PM, Meijers KA, Brand R, et al. Analysis of the synovial cell infiltrate in early rheumatoid synovial tissue in relation to local disease activity. Arthritis Rheum 1997;40:217–25.
5. Jevtic V, Watt I, Rozman B, Presetnik M, Logar D, Praprotnik S, et al. Prognostic value of contrast enhanced Gd-DTPA MRI for development of bone erosive changes in rheumatoid arthritis. Br J Rheumatol 1996;35 Suppl 3:26–30.
6. Felson DT. Choosing a core set of disease activity measures for rheumatoid arthritis clinical trials. J Rheumatol 1993;20:531–4.
7. Kaye JJ. Arthritis: roles of radiography and other imaging techniques in evaluation. Radiology 1990;177:601–8.
8. Lavini C. DCE-MRI analysis package comprising pixel-by-pixel classification of time intensity curves shapes, permeability maps and Gd concentration calculation. MAGMA 2008;21 Suppl 1:486.
9. Tofts PS, Brix G, Buckley DL, Evelhoch JL, Henderson E, Knopp MV, et al. Estimating kinetic parameters from dynamic contrast-enhanced T_1-weighted MRI of a diffusable tracer: standardized quantities and symbols. J Magn Reson Imaging 1999;10:223–32.
10. Cimmino MA, Innocenti S, Livrone F, Magnaguagno F, Silvestri E, Garlaschi G. Dynamic gadolinium-enhanced magnetic resonance imaging of the wrist in patients with rheumatoid arthritis can discriminate active from inactive disease. Arthritis Rheum 2003;48:1207–13.
11. Ostergaard M, Stoltenberg M, Lovgreen-Nielsen P, Volck B, Sonne-Holm S, Lorenzen I. Quantification of synovistis by MRI: correlation between dynamic and static gadolinium-enhanced magnetic resonance imaging and microscopic and macroscopic signs of synovial inflammation. Magn Reson Imaging 1998;16:743–54.
12. Palosaari K, Vuotila J, Takalo R, Jartti A, Niemela R, Haapea M, et al. Contrast-enhanced dynamic and static MRI correlates with quantitative 99Tcm-labelled nanocolloid scintigraphy: study of early rheumatoid arthritis patients. Rheumatology (Oxford) 2004;43:1364–73.
13. Gaffney K, Cookson J, Blake D, Coumbe A, Blades S. Quantification of rheumatoid synovitis by magnetic resonance imaging. Arthritis Rheum 1995;38:1610–7.
14. Tamai K, Yamato M, Yamaguchi T, Ohno W. Dynamic magnetic resonance imaging for the evaluation of synovitis in patients with rheumatoid arthritis. Arthritis Rheum 1994;37:1151–7.
15. Axelsen MB, Stoltenberg M, Poggenborg RP, Kubassova O, Boesen M, Bliddal H, et al. Dynamic gadolinium-enhanced magnetic resonance imaging allows accurate assessment of the synovial inflammatory activity in rheumatoid arthritis knee joints: a comparison with synovial histology. Scand J Rheumatol 2012;41:89–94.
16. Vordenbaumen S, Schleich C, Logters T, Sewerin P, Bleck E, Pauly T, et al. Dynamic contrast-enhanced magnetic resonance imaging of metacarpophalangeal joints reflects histological signs of synovitis in rheumatoid arthritis. Arthritis Res Ther 2014;16:452.
17. Huang J, Stewart N, Crabbe J, Robinson E, McLean L, Yeoman S, et al. A 1-year follow-up study of dynamic magnetic resonance imaging in early rheumatoid arthritis reveals synovitis to be increased in shared epitope-positive patients and predictive of erosions at 1 year. Rheumatology (Oxford) 2000;39:407–16.
18. Kalden-Nemeth D, Grebmeier J, Antoni C, Manger B, Wolf F, Kalden JR. NMR monitoring of rheumatoid arthritis patients receiving anti-TNF-a monoclonal antibody therapy. Rheumatol Int 1997;16:249–55.
19. Ostergaard M, Stoltenberg M, Henriksen O, Lorenzen I. Quantitative assessment of synovial inflammation by dynamic gadolinium-enhanced magnetic resonance imaging: a study of the effect of intra-articular methylprednisolone on the rate of early synovial enhancement. Br J Rheumatol 1996;35:50–9.

20. Reece RJ, Kraan MC, Radjenovic A, Veale DJ, O'Connor PJ, Ridgway JP, et al. Comparative assessment of leflunomide and methotrexate for the treatment of rheumatoid arthritis, by dynamic enhanced magnetic resonance imaging. Arthritis Rheum 2002;46:366–72.
21. Cimmino MA, Parodi M, Zampogna G, Boesen M, Kubassova O, Barbieri F, et al. Dynamic contrast-enhanced, extremity-dedicated MRI identifies synovitis changes in the follow-up of rheumatoid arthritis patients treated with rituximab. Clin Exp Rheumatol 2014;32:647–52.
22. Meier R, Thuermel K, Noel PB, Moog P, Sievert M, Ahari C, et al. Synovitis in patients with early inflammatory arthritis monitored with quantitative analysis of dynamic contrast-enhanced optical imaging and MR imaging. Radiology 2014;270:176–85.
23. Hawighorst H, Knapstein PG, Weikel W, Knopp MV, Zuna I, Knof A, et al. Angiogenesis of uterine cervical carcinoma: characterization by pharmacokinetic magnetic resonance parameters and histological microvessel density with correlation to lymphatic involvement. Cancer Res 1997;57:4777–86.
24. Padhani AR, Gapinski CJ, Macvicar DA, Parker GJ, Suckling J, Revell PB, et al. Dynamic contrast enhanced MRI of prostate cancer: correlation with morphology and tumour stage, histological grade and PSA. Clin Radiol 2000;55:99–109.
25. Galbraith SM, Maxwell RJ, Lodge MA, Tozer GM, Wilson J, Taylor NJ, et al. Combretastatin A4 phosphate has tumor antivascular activity in rat and man as demonstrated by dynamic magnetic resonance imaging. J Clin Oncol 2003;21:2831–42.
26. Kennedy SD, Szczepaniak LS, Gibson SL, Hilf R, Foster TH, Bryant RG. Quantitative MRI of Gd-DTPA uptake in tumors: response to photodynamic therapy. Magn Reson Med 1994;31:292–301.
27. De Hair MJ, Harty LC, Gerlag DM, Pitzalis C, Veale DJ, Tak PP. Synovial tissue analysis for the discovery of diagnostic and prognostic biomarkers in patients with early arthritis. J Rheumatol 2011;38:2068–72.
28. Prevoo ML, van 't Hof MA, Kuper HH, van Leeuwen MA, van de Putte LB, van Riel PL. Modified disease activity scores that include twenty-eight–joint counts: development and validation in a prospective longitudinal study of patients with rheumatoid arthritis. Arthritis Rheum 1995;38:44–8.
29. Aletaha D, Neogi T, Silman AJ, Funovits J, Felson DT, Bingham CO III, et al. 2010 rheumatoid arthritis classification criteria: an American College of Rheumatology/European League Against Rheumatism collaborative initiative. Arthritis Rheum 2010;62:2569–81.
30. Altman R, Asch E, Bloch D, Bole G, Borenstein D, Brandt K, et al. Development of criteria for the classification and reporting of osteoarthritis: classification of osteoarthritis of the knee. Arthritis Rheum 1986;29:1039–49.
31. Altman R, Alarcon G, Appelrouth D, Bloch D, Borenstein D, Brandt K, et al. The American College of Rheumatology criteria for the classification and reporting of osteoarthritis of the hand. Arthritis Rheum 1990;33:1601–10.
32. Dougados M, van der Linden S, Juhlin R, Huitfeldt B, Amor B, Calin A, et al, and the European Spondylarthropathy Study Group. The European Spondylarthropathy Study Group preliminary criteria for the classification of spondylarthropathy. Arthritis Rheum 1991;34:1218–27.
33. Hochberg MC, for the Diagnostic and Therapeutic Criteria Committee of the American College of Rheumatology. Updating the American College of Rheumatology revised criteria for the classification of systemic lupus erythematosus [letter]. Arthritis Rheum 1997;40:1725.
34. Wallace SL, Robinson H, Masi AT, Decker JL, McCarty DJ, Yu TF. Preliminary criteria for the classification of the acute arthritis of primary gout. Arthritis Rheum 1977;20:895–900.
35. Gerlag DM, Raza K, van Baarsen LG, Brouwer E, Buckley CD, Burmester GR, et al. EULAR recommendations for terminology and research in individuals at risk of rheumatoid arthritis: report from the Study Group for Risk Factors for Rheumatoid Arthritis. Ann Rheum Dis 2012;71:638–41.
36. Visser H, le Cessie S, Vos K, Breedveld FC, Hazes JM. How to diagnose rheumatoid arthritis early: a prediction model for persistent (erosive) arthritis. Arthritis Rheum 2002;46:357–65.
37. Schabel MC, Parker DL. Uncertainty and bias in contrast concentration measurements using spoiled gradient echo pulse sequences. Phys Med Biol 2008;53:2345–73.
38. Parker GJ, Roberts C, Macdonald A, Buonaccorsi GA, Cheung S, Buckley DL, et al. Experimentally-derived functional form for a population-averaged high-temporal-resolution arterial input function for dynamic contrast-enhanced MRI. Magn Reson Med 2006;56:993–1000.

39. Lavini C, Verhoeff JJ. Reproducibility of the gadolinium concentration measurements and of the fitting parameters of the vascular input function in the superior sagittal sinus in a patient population. Magn Reson Imaging 2010;28:1420–30.
40. Orton MR, d'Arcy JA, Walker-Samuel S, Hawkes DJ, Atkinson D, Collins DJ, et al. Computationally efficient vascular input function models for quantitative kinetic modelling using DCEMRI. Phys Med Biol 2008;53:1225–39.
41. Gerlag DM, Tak PP. How to perform and analyse synovial biopsies. Best Pract Res Clin Rheumatol 2013;27:195–207.
42. Van de Sande MG, Gerlag DM, Lodde BM, van Baarsen LG, Alivernini S, Codullo V, et al. Evaluating antirheumatic treatments using synovial biopsy: a recommendation for standardisation to be used in clinical trials. Ann Rheum Dis 2011;70:423–7.
43. Kraan MC, Reece RJ, Smeets TJ, Veale DJ, Emery P, Tak PP. Comparison of synovial tissues from the knee joints and the small joints of rheumatoid arthritis patients: implications for pathogenesis and evaluation of treatment. Arthritis Rheum 2002;46:2034–8.
44. Gerlag D, Tak PP. Synovial biopsy. Best Pract Res Clin Rheumatol 2005;19:387–400.
45. Van de Sande MG, de Hair MJ, Schuller Y, van de Sande GP, Wijbrandts CA, Dinant HJ, et al. The features of the synovium in early rheumatoid arthritis according to the 2010 ACR/EULAR classification criteria. PLoS One 2012;7:e36668.
46. Axelsen MB, Ejbjerg BJ, Hetland ML, Skjodt H, Majgaard O, Lauridsen UB, et al. Differentiation between early rheumatoid arthritis patients and healthy persons by conventional and dynamic contrast-enhanced magnetic resonance imaging. Scand J Rheumatol 2014;43:109–18.
47. Konez O, Bis KG, Shirkhoda A, Shetty AN, Gurgun M, Wilcox R, et al. Gradient-echo perfusion imaging of musculoskeletal abnormalities with contrast-enhanced two-dimensional fat-saturation FLASH. J Magn Reson Imaging 1997;7:895–902.
48. Kuhl CK, Mielcareck P, Klaschik S, Leutner C, Wardelmann E, Gieseke J, et al. Dynamic breast MR imaging: are signal intensity time course data useful for differential diagnosis of enhancing lesions? Radiology 1999;211:101–10.
49. Shastry M, Miles KA, Win T, Janes SM, Endozo R, Meagher M, et al. Integrated 18F-fluorodeoxyglucose-positron emission tomography/dynamic contrast-enhanced computed tomography to phenotype non-small cell lung carcinoma. Mol Imaging 2012;11:353–60.
50. Van der Woude HJ, Verstraete KL, Hogendoorn PC, Taminiau AH, Hermans J, Bloem JL. Musculoskeletal tumors: does fast dynamic contrast-enhanced subtraction MR imaging contribute to the characterization? Radiology 1998;208:821–8.
51. Van Rijswijk CS, Hogendoorn PC, Taminiau AH, Bloem JL. Synovial sarcoma: dynamic contrast-enhanced MR imaging features. Skeletal Radiol 2001;30:25–30.
52. Verstraete KL, De Deene Y, Roels H, Dierick A, Uyttendaele D, Kunnen M. Benign and malignant musculoskeletal lesions: dynamic contrast-enhanced MR imaging—parametric "first-pass" images depict tissue vascularization and perfusion. Radiology 1994;192:835–43.
53. Harry VN, Semple SI, Parkin DE, Gilbert FJ. Use of new imaging techniques to predict tumour response to therapy. Lancet Oncol 2010;11:92–102.
54. Fearon U, Griosios K, Fraser A, Reece R, Emery P, Jones PF, et al. Angiopoietins, growth factors, and vascular morphology in early arthritis. J Rheumatol 2003;30:260–8.
55. Veale D, Yanni G, Rogers S, Barnes L, Bresnihan B, FitzGerald O. Reduced synovial membrane macrophage numbers, ELAM-1 expression, and lining layer hyperplasia in psoriatic arthritis as compared with rheumatoid arthritis. Arthritis Rheum 1993;36:893–900.
56. Cuenod CA, Fournier L, Balvay D, Guinebretiere JM. Tumor angiogenesis: pathophysiology and implications for contrast-enhanced MRI and CT assessment. Abdom Imaging 2006;31:188–93.
57. Carmeliet P. Angiogenesis in life, disease and medicine. Nature 2005;438:932–6.
58. Lavini C. Simulating the effect of input errors on the accuracy of Tofts' pharmacokinetic model parameters. Magn Reson Imaging 2015;33:222–35.

Supplemental material

Table S8.1 Dynamic contrast-enhanced magnetic resonance imaging pharmacokinetic parameters in different diagnostic and arthritis outcome groups.

A

	RA (n=14)	UA (n=22)	SpA (n=6)	Other (n=5)	*P* value
K^{trans}, min^{-1} (median (IQR))	0.026 (0.008-0.044)	0.028 (0.015-0.042)	0.050 (0.041-0.069)	0.003 (0.000-0.036)	0.026
K_{ep}, min^{-1} (median (IQR))	0.072 (0.018-0.141)	0.162 (0.082-0.195)	0.207 (0.097-0.259)	0.003 (0.001-0.135)	0.024
v_e (no units) (median (IQR))	0.143 (0.088-0.236)	0.172 (0.133-0.230)	0.359 (0.177-0.503)	0.048 (0.009-0.270)	0.094

B

	Self-limiting (n=3)	*Persistent nonerosive* (n=5)	*Erosive disease* (n=3)	*P* value
K^{trans}, min^{-1} (median (IQR or range))	0.006 (0.005-0.022)	0.041 (0.024-0.045)	0.027 (0.000-0.083)	0.212
K_{ep}, min^{-1} (median (IQR or range))	0.033 (0.007-0.117)	0.137 (0.044-0.213)	0.120 (0.000-0.138)	0.262
v_e (no units) (median (IQR or range))	0.078 (0.073-0.176)	0.186 (0.136-0.237)	0.232 (0.001-0.384)	0.357

Parameters are described as median (interquartile range) as appropriate. In **A**, the median (IQR) K^{tran}, $k_{ep,}$ and v_e of patients with early arthritis who were classified as rheumatoid arthritis (RA), unclassified arthritis (UA), spondyloarthritis (SpA), or other arthritides at baseline. In **B,** the median (IQR) K^{tran}, $k_{ep,}$ and v_e per arthritis outcome group (*self-limiting disease*, *persistent nonerosive disease*, or *erosive disease)* in patients fulfilling the ACR/EULAR 2010 criteria for RA after 2 years of followup.

Table S8.2 Severity of swelling of the biopsied joint per diagnosis.

Diagnosis	Severity of swelling biopsied joint (n=47; 0-3 median (IQR))
RA (median (IQR)) (n=14)	1 (0-1)
UA (median (IQR)) (n=22)	2 (1-2)
SpA (median (IQR)) (n=6)	2 (1-2)
Other (median (IQR)) (n=5)	1 (1-1)

Parameters are described as median (interquartile range) as appropriate. RA = rheumatoid arthritis, UA = unclassified arthritis, SpA = spondyloarthritis.